Information Fusion 42 (2018) 179–189

Contents lists available at ScienceDirect

Information Fusion

journal homepage: www.elsevier.com/locate/inffus

Entrotaxis as a strategy for autonomous search and source reconstruction in turbulent conditions

Michael Hutchinson[a], Hyondong Oh[*,b], Wen-Hua Chen[a]

[a] Department of Aeronautical and Automotive Engineering, Loughborough University, Leicestershire, UK
[b] School of Mechanical and Nuclear Engineering, Ulsan National Institute of Science and Technology, Ulsan, Republic of Korea

ARTICLE INFO

Keywords:
Autonomous search
Sensor management
Bayesian inference
Sequential Monte Carlo
Dispersion modelling
Turbulent flow

ABSTRACT

This paper proposes a strategy for performing an efficient autonomous search to find an emitting source of sporadic cues of noisy information. We focus on the search for a source of unknown strength, releasing particles into the atmosphere where turbulence can cause irregular gradients and intermittent patches of sensory cues. Bayesian inference, implemented via the sequential Monte Carlo method, is used to update posterior probability distributions of the source location and strength in response to sensor measurements. Posterior sampling is then used to approximate a reward function, leading to the manoeuvre to where the entropy of the predictive distribution is the greatest. As it is developed based on the maximum entropy sampling principle, the proposed framework is termed as Entrotaxis. We compare the performance and search behaviour of Entrotaxis with the popular Infotaxis algorithm, for searching in sparse and turbulent conditions where typical gradient-based approaches become inefficient or fail. The algorithms are assessed via Monte Carlo simulations with simulated data and an experimental dataset. Whilst outperforming the Infotaxis algorithm in most of our simulated scenarios, by achieving a faster mean search time, the proposed strategy is also more computationally efficient during the decision making process.

1. Introduction

The search for an emitting source of weak, intermittent or noisy signals is an important task for mankind and the natural world. Within the animal kingdom, maximising searching efficiency is of great importance where food sources can be sparse and the mating race is competitive. Autonomous searching strategies have several applications that can benefit civilisation, where a recent example is the search for the missing passenger aircraft, Malaysia Airlines flight MH370 [1].

Optimising the efficiency of search paths is vital when rapid search times have the potential to save lives, for instance: searching for a hazardous toxic gas, localising explosive mines [2], search and rescue missions [3], and even diagnosing medical conditions [4]. Other applications include: locating a lost piece of equipment [5], resource exploration [6] and space exploration [7]. In this paper, we focus on the search and source term estimation of a hazardous source of unknown strength, dispersing in a turbulent medium. Source term estimation is an ill-posed, highly non-linear inverse problem where the strength and location of a source are estimated by fusion of prior information, sensory data, and mathematical models. Reconstruction of the source term enables prediction of the future extent of hazardous contamination, with applications in emergency response following an accidental or deliberate release of harmful chemical, biological, radiological or nuclear (CBRN) material [8].

Searching strategies are adapted to capitalise upon the availability of sensing cues or prior information. In the absence of information or cues, it is common to execute a systematic or random search. Systematic search paths, such as parallel sweep and Archimedean spiral [9], are effective methods provided that the target of interest is stationary, there is no available information, and if efficiency is not the priority. In early works of search theory, systematic searches were studied by the US navy, to optimise aircraft flight paths whilst hunting submarines [9]. In the animal kingdom systematic trajectories are rarely observed, nonetheless there is evidence to suggest that desert ants follow an Archimedean spiral path whilst foraging [10]. Random searches can be argued to be the most prevalent in nature. For instance, Albatrosses, among many other species, have been observed to display lévy flight patterns [11] whilst hunting. A large dataset of the movement of open-ocean predatory fish provides supporting evidence that hunters follow lévy patterns where prey is sparse, although it is suggested Brownian motion is observed when prey is abundant [12]. Regardless, the lévy hypothesis is a source of dispute within the literature

* Corresponding author.
E-mail addresses: m.hutchinson2@lboro.ac.uk (M. Hutchinson), h.oh@unist.ac.kr (H. Oh), w.chen@lboro.ac.uk (W.-H. Chen).

https://doi.org/10.1016/j.inffus.2017.10.009
Received 15 March 2017; Received in revised form 24 August 2017; Accepted 29 October 2017
Available online 06 November 2017

and alternative hypotheses may be more probable [13].

When prior knowledge or sensing cues are available, the search strategy is adapted to exploit the extra information. Chemotaxic strategies use concentration gradients to direct motion towards an emitting source. Bacteria, such as Escherichia coli, use Chemotaxis to move towards the greatest supply of energy by slowly climbing positive concentration gradients [14]. However, in sparse sensing conditions, which can be caused by a weak source, large distances or turbulent mixing, Chemotaxic strategies are abandoned as irregular gradients and intermittent sensing cause them to lose performance or fail. Anemotaxis concerns the use of wind information to help guide the searcher, a strategy which has been observed in honeybees [15] and the male silkworm moth [16], among others.

Most aforementioned biologically-inspired search strategies can be regarded as reactive, where observations trigger predefined movement sequences to localise a source [17,18]. Alternatively, approaches have been developed based on information-theoretic principles, otherwise known as cognitive strategies. Information theory was first applied to the search problem to optimise effort during aerial reconnaissance [19]. The Shannon entropy, from the theory of information and communication, was used to compare the effectiveness of different pre-planned strategies. Recent cognitive search strategies make decisions on-line, formulated as a partially-observable Markov decision process (POMDP) [20]. The POMDP framework utilises state, action and reward. For our problem, the state refers to the current knowledge about the source, the actions are movements towards potential future measurement locations and the reward is a quantity to describe the gain in information supplied by the corresponding action. Infotaxis is a cognitive search strategy proven to be effective in the sparse sensing conditions where gradient based approaches would be unsuitable [21]. By assuming environmental parameters and the source strength were known, Bayes rule was applied to update a probabilistic map of source location throughout the search, in response to sparse sensory cues in the form of particle encounters with a sensor [22]. Considering one-step ahead manoeuvres on a square lattice, the most informative actions were selected based on minimising the expected entropy of the posterior distribution, with an adaptive term to bias the searcher's movements towards the source as levels of uncertainty were reduced. The strategy showed robustness to significantly sparse conditions and has thus inspired several studies proposing modifications and extensions [23,24]. A critical extension of the algorithm was its implementation in the sequential Monte Carlo framework, using a particle filter, alleviating its grid based implementation and allowing the source strength to be included as a parameter to be estimated [25]. Several reward functions were compared including an Infotaxic II reward, which removed the Infotaxis' bias towards the source, and a reward based on the Bhattacharyya distance. Although the differences among strategies were marginal, the Infotaxis II reward slightly outperformed the others in numerical simulations.

Perhaps the strongest argument that favours a reactive search strategy over the cognitive approach is the higher computational cost of the cognitive search. Aside from the possible complexity of the underlying dispersion and sensor models, the cognitive strategies require a new posterior distribution to be calculated, for each possible future measurement, at each considered location. This could pose a serious problem in conditions where the number of possible measurements or actions increases, or in the development of multiple-step ahead or collaborative multi-agent search strategies. Despite the computational burden, cognitive strategies are preferred due to their probabilistic nature. They have been shown to be more robust in sparse conditions [18], and additional parameters (such as the source strength and potentially the time of release) can be estimated. The latter falls into the domain of source term estimation, reviewed in [8]. Typically, source term estimation or reconstruction is performed using a network of static concentration sensors. Observations are fused with meteorological data and a dispersion model in order to gain a point estimate or posterior probability density function of source parameters through optimisation [26,27] or Bayesian inference [28] algorithms. The cognitive search formulation has enabled information-driven control for source estimation using a mobile sensor [29].

This paper proposes an alternative cognitive search and source term estimation strategy, termed as Entrotaxis. Similar to previous work [25], the sequential Monte Carlo framework is used to update probability distributions of source parameters. Maximum entropy sampling principles are newly used to guide the searcher [30], hence we coined the name 'Entrotaxis' by following the name convention in the literature [21,25]. The approach follows a similar procedure to Infotaxis II [25] in a way that the probabilistic representation of the source is used; however, the reward function considers the entropy of the predictive measurement distribution as opposed to the entropy of the expected posterior. Essentially, Entrotaxis will guide the searcher to where there is the most uncertainty in the next measurement, while Infotaxis will move the searcher to where the next measurement is expected to minimise the uncertainty in the posterior distribution. The maximum entropy sampling principles upon which the algorithm is built are rather intuitive, where it is considered the most is learnt by sampling from where the least is known. This approach has proven to be effective in the literature on optimal Bayesian experimental design [30]. Whilst outperforming the Infotaxis algorithm in several conditions by more rapidly localising the source, the proposed Entrotaxis strategy is also slightly more computationally efficient as hypothesised posterior distributions do not have to be computed in the decision making.

The remainder of this paper is organised as follows. In Section 2, we formulate the problem, including mathematical equations that model the spread of emitted particles and the number of particle encounters with the sensor. In Section 3, the conceptual solution of the Entrotaxis algorithm is described, covering parameter estimation and mobile sensor control. In Section 4, we describe the sequential Monte Carlo implementation of the Entrotaxis algorithm. In Section 5, an illustrative run is presented, the Infotaxis II algorithm is briefly described, and numerical simulations compare the difference in performance and search characteristics between the two strategies. The results using an experimental dataset are given in Section 6, and finally, Section 7 presents conclusions and future work.

2. Problem description

The autonomous search algorithm is to guide a searcher to localise and reconstruct the source of a constant emission of particles characterised by the unknown source term vector $\theta_s = [\mathbf{r}_s\ Q_s]^\mathsf{T}$, where $Q_s \in \mathsf{R}^+$ is the emission rate of the source located at $\mathbf{r}_s = [X_s\ Y_s]^\mathsf{T} \in \Omega$, where $\Omega \subset \mathsf{R}^2$ denotes the search area. The autonomous searching agent located at $\mathbf{p}_k = [x_k\ y_k]^\mathsf{T} \in \Omega$ and equipped with a particle detector of area a, is to navigate the environment, choosing from the admissible set of actions $U_k = \{\uparrow, \downarrow, \leftarrow, \rightarrow\}$, the move $\mathbf{u}_k^* \in U_k$ that is expected to yield the most information.

The searcher shall collect measurements in the form of the number of particle encounters $d \in \mathsf{Z}^+$ with the sensor. The particles emitted from the source disperse through the domain under turbulent transport conditions. We adopt the three dimensional model $R(\mathbf{p}_k|\theta_s)$ presented in [21], to denote the rate of particles encountered by a spherical sensor of radius a at position $\mathbf{p}_k$ from the source defined by the source term vector θ_s. Particles emitted from the source have a finite lifetime τ, propagate with isotropic effective diffusivity σ (which approximates the combined effect of turbulent and molecular diffusion) and are advected by a mean current or wind v [21]. Adopting a sign convention that sets the wind in the direction of the negative y axis yields the analytical solution:

$$R(\mathbf{p}_k|\theta_s) = \frac{aQ_s}{\|\mathbf{p}_k - \mathbf{r}_s\|} \exp\left[\frac{-\|\mathbf{p}_k - \mathbf{r}_s\|}{\lambda}\right] \exp\left[\frac{-(y_k - Y_s)v}{2\sigma}\right], \tag{1}$$

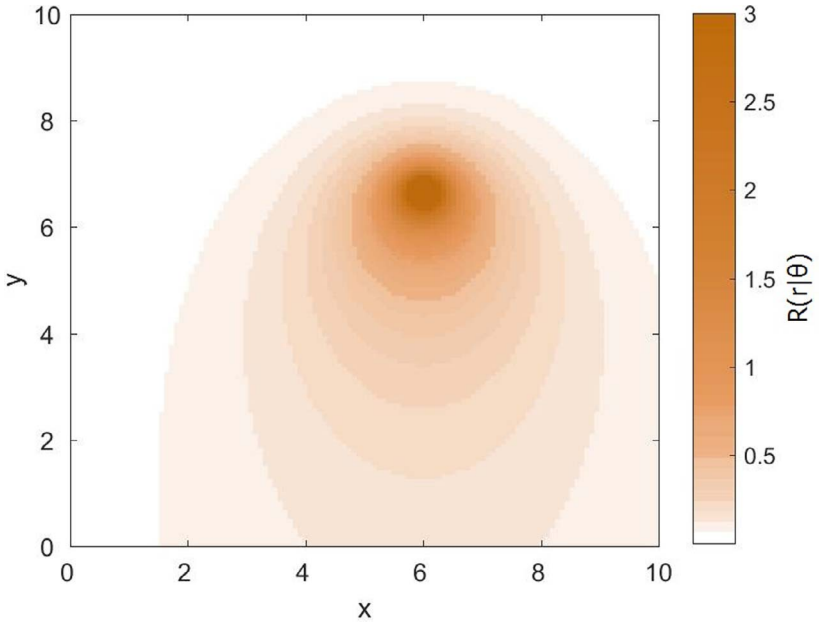

Fig. 1. The mean rate of particle encounters with a sensor of size $a = 1$ after time interval $t_0 = 1$ and parameters $Q_s = 1$, $X_s = 6$, $Y_s = 6.67$, $v = 1$, $\tau = 250$ and $\sigma = 1$.

where

$$\lambda = \sqrt{\frac{\sigma\tau}{1 + \frac{v^2\tau}{4\sigma}}}. \tag{2}$$

The mean number of particle encounters expected by the sensor is simply the product of the rate of encounters and the sampling time $\mu_k = R(\mathbf{p}_k|\theta_s)t_0$. An example plot of the mean rate of encounters is given in Fig. 1.

The stochastic process of particle encounters with the sensor, given the mean rate, is modelled by a Poisson distribution [21] which denotes the probability that the sensor located at $\mathbf{p}_k$ will encounter $d_k \in \mathbb{Z}^+$ particles during the sampling time interval t_0 as given:

$$P(d_k|\mu_k) = \frac{\mu_k^{d_k}}{d_k!}e^{-\mu_k}. \tag{3}$$

We illustrate an example of what the searcher may observe at a fixed point in time in Fig. 2, by running the Poisson sensor model over the mean rate of particle encounters from Fig. 1. The plot demonstrates the significant challenge imposed on source localisation by sparse and turbulent conditions.

We assume that the average particle lifetime τ and the environmental parameters σ and v are known, with the source term vector θ_s remaining to be estimated.

3. Conceptual solution

The proposed Entrotaxis algorithm consists of estimation of the source parameter vector θ_s, followed by an analysis to determine the most informative manoeuvre for a mobile sensor. Estimation is carried out using the Bayesian framework to estimate the source parameters in the presence of uncertainty. Information theory is used to identify the most informative manoeuvre, which is defined as the location where the entropy of the predictive distribution is at its maximum. In other words, the searcher moves to the position where the least is known about the next measurement. This is the maximum entropy sampling

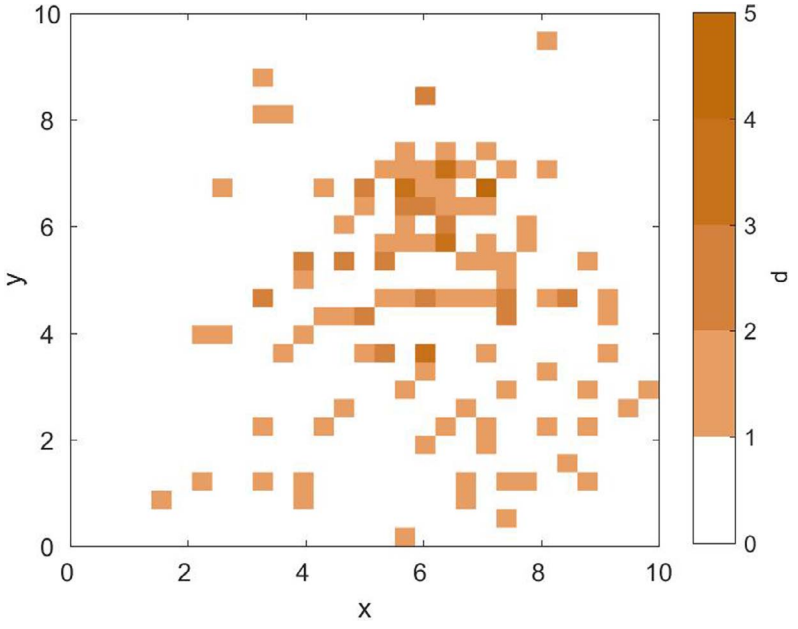

Fig. 2. Example number of particles encountered d by the sensor at searcher nodes, obtained by running the Poisson sensor model on Fig. 1.

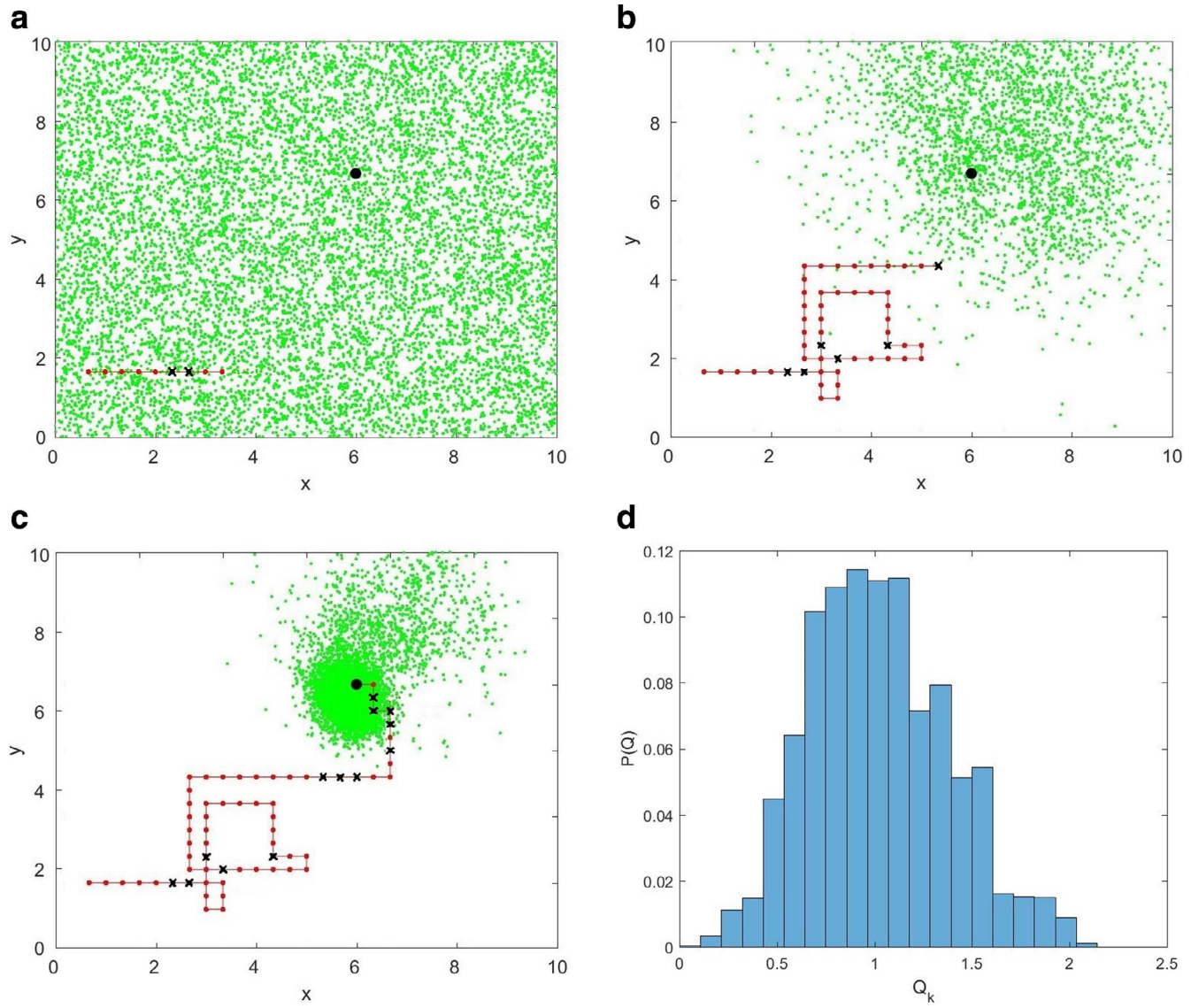

Fig. 3. An illustrative run of the Entrotaxis algorithm at time steps: a) $k = 9$; b) $k = 41$; and c) $k = 71$. The histogram in d) displays the posterior estimate of the source release rate Q_k at the end of the search. Simulation parameters are as follows: $[x_1\ y_1] = [0.67\ 1.67]$, $X_s = 6$, $Y_s = 6.67$, $Q_s = 1$, $v = 1$, $a = 1$, $\tau = 250$, $\sigma = 1$, $N = 10,000$. The true source location is indicated by a large black dot, green dots represent the random samples of the particle filter, the red line indicates the trajectory of the searcher, red dots indicate zero measurements and black crosses non-zero measurements. (For interpretation of the references to colour in this figure legend, the reader is referred to the web version of this article.)

principle, which has been popular in research on optimal design of experiments [30].

3.1. Estimation

We use a probabilistic framework to estimate the source parameters in response to uncertain information, in the form of particle encounters with a sensor. The current state of knowledge regarding the parameters is represented by a posterior probability density function (PDF) $P(\theta_k|\mathbf{D}_{1:k})$, where $\mathbf{D}_{1:k}$: $=\{d_i(\mathbf{p}_i),\ldots,d_k(\mathbf{p}_k)\}$ refers to the measurement data at visited locations. The posterior PDF is subsequently updated according to Bayes rule as sensory data are acquired:

$$P(\theta_k|\mathbf{D}_{1:k}) = \frac{P(\theta_k|\mathbf{D}_{1:k-1})P(d_k(\mathbf{p}_k)|\theta_k)}{P(d_k(\mathbf{p}_k)|\mathbf{D}_{1:k-1})}, \tag{4}$$

where

$$P(d_k(\mathbf{p}_k)|\mathbf{D}_{1:k-1}) = \int P(\theta_k|\mathbf{D}_{1:k-1})P(d_k(\mathbf{p}_k)|\theta_k,)\,\mathrm{d}\theta_k. \tag{5}$$

If information concerning the source term is available prior to the search, it can be exploited through an appropriate distribution to represent the prior knowledge known about the release. However, in the absence of information, the initial prior distribution $\pi(\theta_0) \equiv P(\theta_0)$ can be set to an uninformative distribution. In this work, we use a uniform distribution that is bounded by the domain Ω, unless otherwise stated, assuming no prior information is available. In subsequent iterations, the prior distributions are replaced to reflect the information gained from the previous sequence.

The likelihood function approximates the probability of the observed data $d_k(\mathbf{p}_k)$, given a hypothesised source parameter estimate θ_k. We adopt the Poisson sensor model Eq. (3) for the likelihood function:

$$P(d_k(\mathbf{p}_k)|\theta_k) = \frac{(R(\mathbf{p}_k|\theta_k)t_0)^{d_k(\mathbf{p}_k)}}{d_k(\mathbf{p}_k)!}e^{-R(\mathbf{p}_k|\theta_k)t_0}, \tag{6}$$

where $R(\mathbf{p}_k|\theta_k)$ is the inferred mean rate of particle encounters. The Bayesian estimation of source parameters is implemented in the sequential Monte Carlo framework using a particle filter [31], which will be described in Section 4.

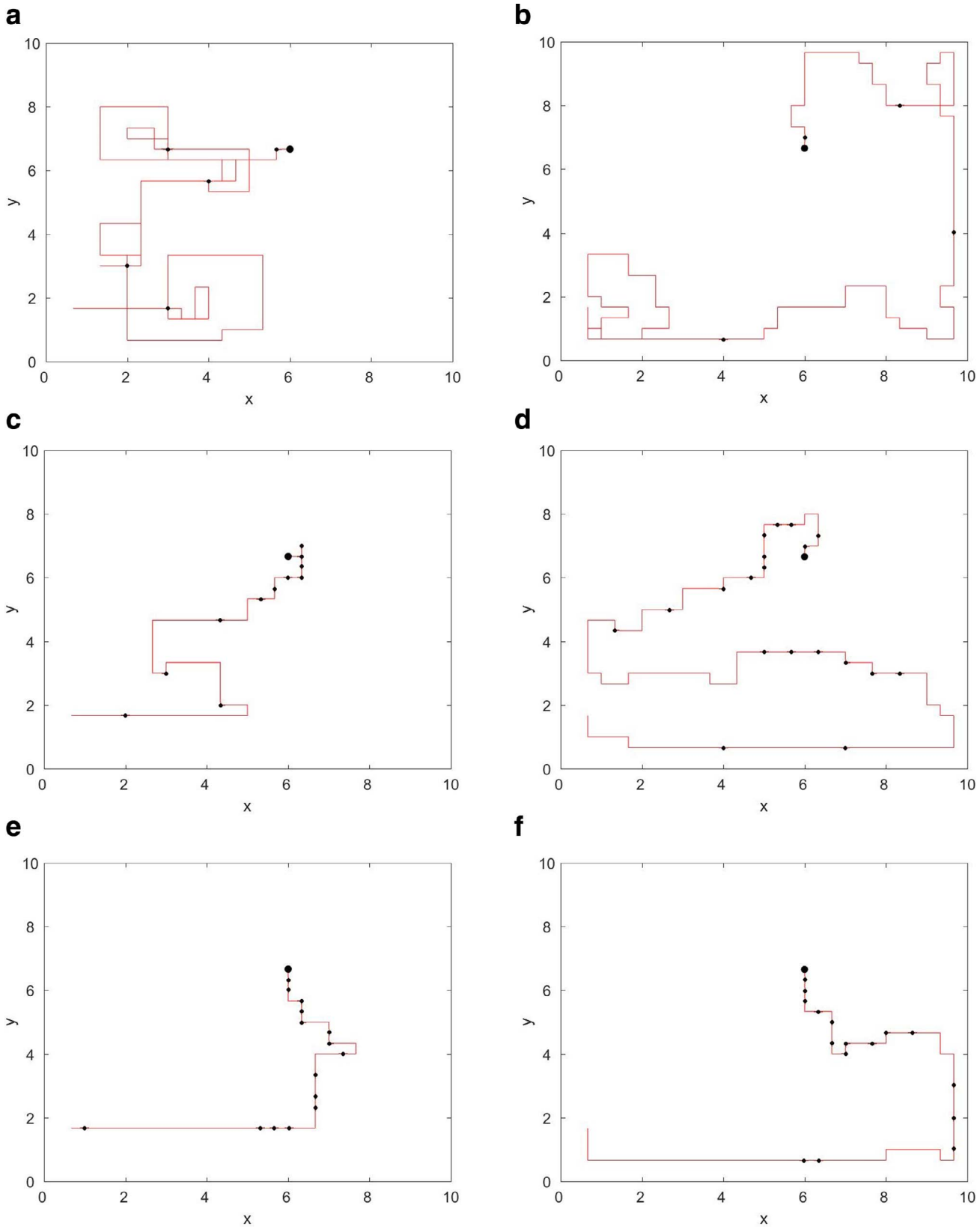

Fig. 4. Search paths of Entrotaxis (left) and Infotaxis (right) strategies subject to various release rates: a,b) $Q_s = 0.2$; c,d) $Q_s = 1$; e,f) $Q_s = 2$.

Table 1
Performance comparison for different values of release rate Q_s for 100 Monte Carlo simulations. (SR = success rate [%]; MST = mean search time [number of measurements]).

Q_s	0.1	0.2	0.5	1	2	4
Entrotaxis						
SR	100	99	100	99	100	100
MST	196	140	96	79	62	49
Infotaxis II						
SR	100	99	100	100	100	99
MST	273	187	129	105	81	67

3.2. Decision making for mobile sensor control

The goal of sensor control is to choose the manoeuvre $\mathbf{u}_k^*$ from an admissible set of actions $U_k = \{\uparrow, \downarrow, \leftarrow, \rightarrow\}$, that is expected to yield the most information $I(\mathbf{u}_k)$, as given:

$$\mathbf{u}_k^* = \arg\max_{\mathbf{u}_k \in U_k} \{I(\mathbf{u}_k)\}. \tag{7}$$

In Eq. (7), the expected information $I(\mathbf{u}_k)$ is defined from maximum entropy sampling principles as the manoeuvre to the position where the entropy of the predictive distribution is the greatest. This strategy is adapted from the literature on Bayesian experimental design [30]. Note that, in the widely-used Infotaxis strategy, it was common to offer an option to remain at the current position [21,25]. Adhering to the fundamentals of maximum entropy sampling, where we wish to sample from the position of the greatest level of uncertainty, this option has been removed.

In this work, we use the Shannon entropy $H(\cdot)$ as the expected information measure, resulting in:

$$I(\mathbf{u}_k) = -\int P(\hat{d}_{k+1}(\hat{\mathbf{p}}_{k+1})|\mathbf{D}_{1:k}) \log P(\hat{d}_{k+1}(\hat{\mathbf{p}}_{k+1})|\mathbf{D}_{1:k})\, \mathrm{d}\hat{d}_{k+1}, \tag{8}$$

where $\hat{d}_{k+1}(\hat{\mathbf{p}}_{k+1})$ refers to the unknown measurement at the potential sampling position $\hat{\mathbf{p}}_{k+1}$. Until the manoeuvre is made, this data is unknown. The method applied to approximate Eq. (8) will be described in the decision making implementation in Section 4.

The sensor control strategy provides the full search algorithm under a single framework, which provides balanced exploration and exploitation by adapting to the state of the posterior PDF of source parameters. The approach naturally moves towards the source location, as the posterior estimate becomes more certain.

4. Implementation

We implement the Bayesian estimation of source parameters in the sequential Monte Carlo framework using a particle filter. The output is an approximation of the posterior distribution $P(\theta_k|\mathbf{D}_{1:\,k})$, which represents the current state of knowledge about the source parameters. Given the posterior distribution in the form of a weighted sample of particles (which we shall refer to as random samples to avoid confusion with emitted particles from the source), we are able to approximate the integral in Eq. (8) and select the expected most informative manoeuvre.

4.1. Estimation

We implement the conceptual estimation of source parameters using a particle filter. The posterior from Eq. (4) is approximated by a set of N weighted samples $\{(\theta_k^{(i)}, w_k^{(i)})\}_{1\le i\le N}$, where $\theta_k^{(i)}$ is a point estimate representing a potential source term and $w_k^{(i)}$ is its corresponding normalised weighting such that $\sum_{i=1}^N w_k^{(i)} = 1$. Given the weighted samples, the posterior distribution can be approximated as:

$$P(\theta_k|\mathbf{D}_{1:k}) \approx \sum_{i=1}^{N} w_k^{(i)} \delta(\theta - \theta_k^{(i)}), \tag{9}$$

where $\delta(\cdot)$ is the Dirac delta function. We update the sample weights in a recursive manner by sequential importance sampling. At each time step, a new sample $\theta_k^{(i)}$ is drawn from the proposal distribution $q(\theta_k^{(i)})$, which should resemble $P(\theta_k|\mathbf{D}_{1:\,k})$. Corresponding sample weights are then updated according to:

$$\overline{w}_k^{(i)} = w_{k-1}^{(i)} \cdot \frac{P(\theta_k^{(i)}|\theta_{k-1}^{(i)}) P(d_k(\mathbf{p}_k)|\theta_k^{(i)})}{q(\theta_k^{(i)}|\theta_{k-1}^{(i)}, d_k)}. \tag{10}$$

By assuming a time-invariant source term (i.e. the source position is fixed and the emission rate is constant), we can assume the proposal distribution is equal to the posterior at time $k-1$, i.e. $q(\theta_k^{(i)}) = P(\theta_{k-1}|\mathbf{D}_{1:k-1})$. This leads to a simple algorithm where $\theta_k^{(i)} = \theta_{k-1}^{(i)}$ for $i = 1, \ldots, N$ [25]. Due to cancellation of terms in Eq. (10), the un-normalised particle weights are updated using the likelihood function and the previous weight as follows:

$$\overline{w}_k^{(i)} = w_{k-1}^{(i)} \cdot P(d_k(\mathbf{p}_k)|\theta_k^{(i)}). \tag{11}$$

We then normalise the sample weights $w_k^{(i)} = \overline{w}_k^{(i)} / \sum_{i=1}^N \overline{w}_k^{(i)}$ to obtain the new approximation of the posterior.

Importance sampling is carried out sequentially at each time step. To avoid sample degeneracy, we re-sample when the number of effective point estimates falls below a pre-specified threshold η. To improve sample diversity, re-sampled estimates are subject to a Markov chain Monte Carlo move step [31].

4.2. Decision making for mobile sensor control

To solve Eq. (8) when the future measurement $\hat{d}_{k+1}$ is unknown, we can approximate the probability of the expected number of particle encounters $P(\hat{d}_{k+1}(\hat{\mathbf{p}}_{k+1})|\mathbf{D}_{1:k})$ at position $\hat{\mathbf{p}}_{k+1}$ using the posterior distribution of source parameters. In other words, we predict what the future measurement may be by using the knowledge currently available about the source:

$$P(\hat{d}_{k+1}(\hat{\mathbf{p}}_{k+1})|\mathbf{D}_{1:k}) \approx \int P(\hat{d}_{k+1}(\hat{\mathbf{p}}_{k+1})|\theta_k) P(\theta_k|\mathbf{D}_{1:k})\, \mathrm{d}\theta_k. \tag{12}$$

This integral can be solved using the weighted sample approximation of the posterior $\{(\theta_k^{(i)}, w_k^{(i)})\}_{1\le i\le N}$. The first term on the right hand side can be obtained using Eq. (6), by replacing the measured data with potential data at the new position. The second term is the corresponding normalized particle weight $\{w_k^{(i)}\}$, resulting in:

$$P(\hat{d}_{k+1}(\hat{\mathbf{p}}_{k+1})|\mathbf{D}_{1:k}) \approx \sum_{i=1}^{N} \frac{(R(\hat{\mathbf{p}}_{k+1}|\theta_k^{(i)}) t_0)^{\hat{d}_{k+1}(\hat{\mathbf{p}}_{k+1})}}{\hat{d}_{k+1}(\hat{\mathbf{p}}_{k+1})!} e^{-R(\mathbf{p}_k|\theta_k^{(i)}) t_0} \cdot w_k^{(i)}. \tag{13}$$

Substituting this into Eq. (8), the entropy for the manoeuvre $I(\mathbf{u}_k)$ can be approximated by a summation over all possible future measurements $\hat{d}_{k+1} = \{0, 1, 2, \ldots, \hat{d}^{\max}\}$:

$$I(\mathbf{u}_k) \approx \sum_{\hat{d}_{k+1}=0}^{\hat{d}^{max}} P(\hat{d}_{k+1}(\hat{\mathbf{p}}_{k+1})|\mathbf{D}_{1:k}) \log P(\hat{d}_{k+1}(\hat{\mathbf{p}}_{k+1})|\mathbf{D}_{1:k}). \tag{14}$$

The expected information I is calculated for each manoeuvre of the set U_k, and the maximum is selected in accordance to Eq. (7). The complete Entrotaxis algorithm is described in Algorithm 1. The stopping criteria (step 16) of the search can be set with regards to the spread of the posterior distribution or a maximum number of search steps.

5. Numerical simulations

In this section, we provide an example run of the Entrotaxis algorithm using simulated data in order to illustrate the estimation and decision making process of the searcher. Monte Carlo simulation results under various conditions are provided to validate the performance of the Entrotaxis search strategy in comparison to the Infotaxis approach [25].

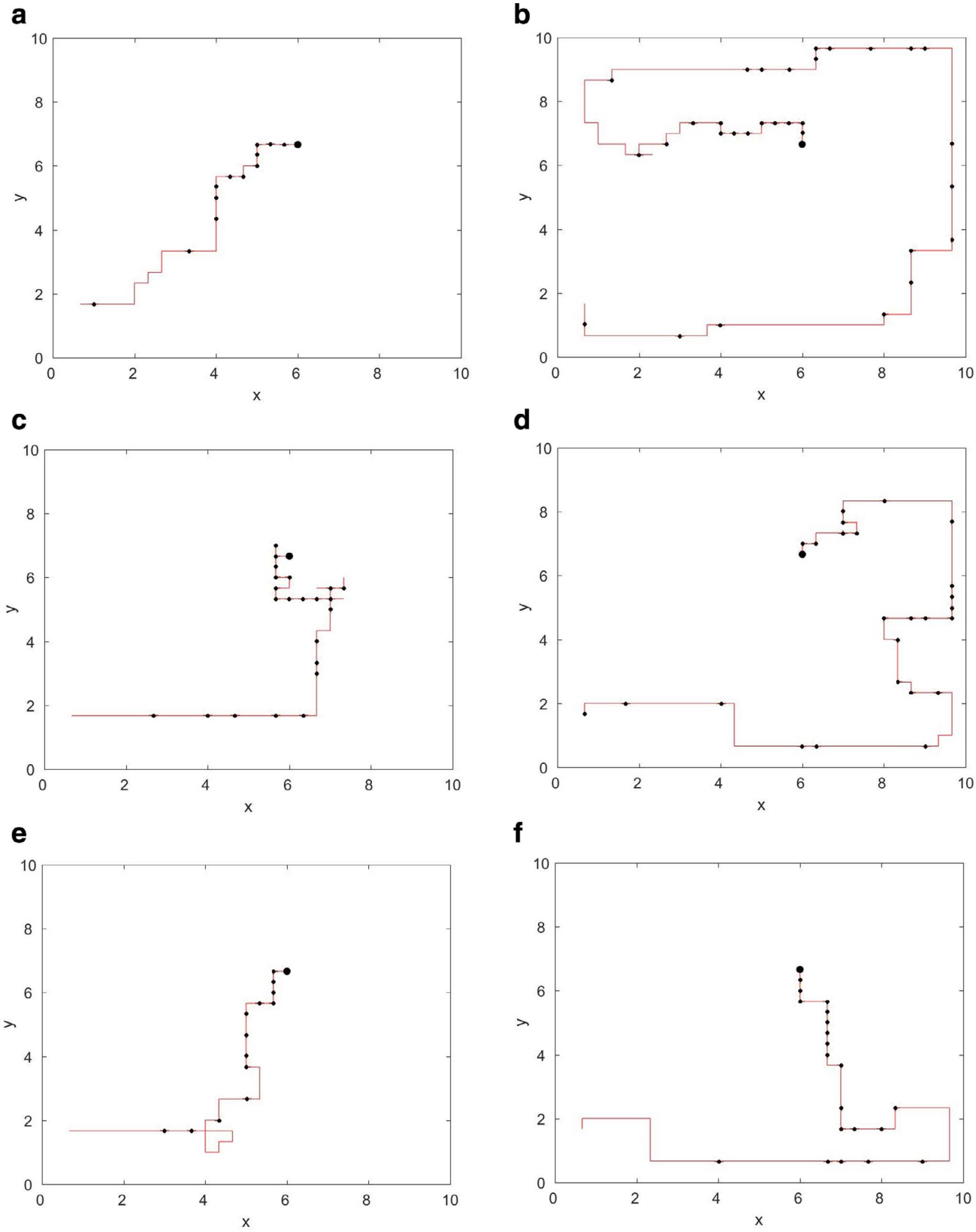

Fig. 5. Search paths of Entrotaxis (left) and Infotaxis (right) strategies subject to various wind velocities: a,b) $v = 0$; c,d) $v = 0.5$; e,f) $v = 1.5$.

Table 2
Search performance for different values of wind velocity V for 100 Monte Carlo simulations. (SR = success rate [%]; MST = mean search time [number of measurements]).

v	0	0.25	0.5	1	1.5
Entrotaxis					
SR	100	100	99	100	99
MST	50	56	58	57	54
Infotaxis II					
SR	100	100	99	100	100
MST	103	99	87	79	75

Table 3
Performance comparison with random starting and source positions. The results after 500 Monte Carlo simulations are shown for various release rate Q_s and wind velocity V combinations.(SR = success rate [%]; MST = mean search time [number of measurements]).

Q_s	0.1	0.1	0.5	0.5	1	1	2	2
v	0	1	0	1	0	1	0	1
Entrotaxis								
SR	100	100	100	100	99.4	99.8	100	99.4
MST	197	180	92	73	68	59	58	50
Infotaxis II								
SR	100	100	99.6	99.6	99.2	99.8	100	99.8
MST	235	237	133	114	101	82	81	66

5.1. Illustrative run

An example of a typical search carried out by the algorithm at various simulations steps is shown in Fig. 3. Simulation parameters used to generate the example are as follows: $X_s = 6$, $Y_s = 6.67$, $Q_s = 1$, $v = 1$, $a = 1$, $\tau = 250$, $\sigma = 1$, $N = 10,000$. We assumed uniform priors within reasonable bounds for the source location and release rates: $\pi(X_0) = \pi(Y_0) = \mathscr{U}[0, 10]$ and $\pi(Q_0) = \mathscr{U}[0, 4]$. The searcher, starting from $[x_1\ y_1] = [0.67\ 1.67]$, begins by moving in a cross wind direction. Upon detection an emitted particle, represented by a black cross on the red path, it is typical for the searcher to circulate around the nearby area. This behaviour, demonstrated in Fig. 3(b), can be considered rational because in very sparse conditions, the most likely source position will initially be where a particle is detected. Furthermore, observations have shown a similar search pattern, commonly performed by the male silkworm moth [32]. Once the searcher has circulated the particle, in response to subsequent null sensor readings, it proceeds to search elsewhere for the source. This behaviour is conducted autonomously, during decision making under the single Entrotaxis framework. The random samples approximating the posterior distribution of the source location are represented by the green dots, and the sequence of figures illustrates how the spread of the samples is decreased throughout the search. This is achieved by updating the sample weightings in response to new data, in the form of sporadic cues of particle encounters with the sensor, and subsequently re-sampling with a focus around highly weighted areas. The histogram in Fig. 3(d) displays the final estimate of the release rate Q_k.

5.2. Monte Carlo simulations

Monte Carlo simulations are run to compare the performance of the Entrotaxis and Infotaxis algorithms. The mathematical formulation of the Infotaxis algorithm is first described and the computational benefit of the Entrotaxis algorithm is assessed. We then briefly discuss the paths taken by the algorithms and evaluate the search performance of the techniques under various conditions with Monte Carlo simulation results.

5.2.1. Infotaxis

We briefly describe the Infotaxis II reward described in [25]. This

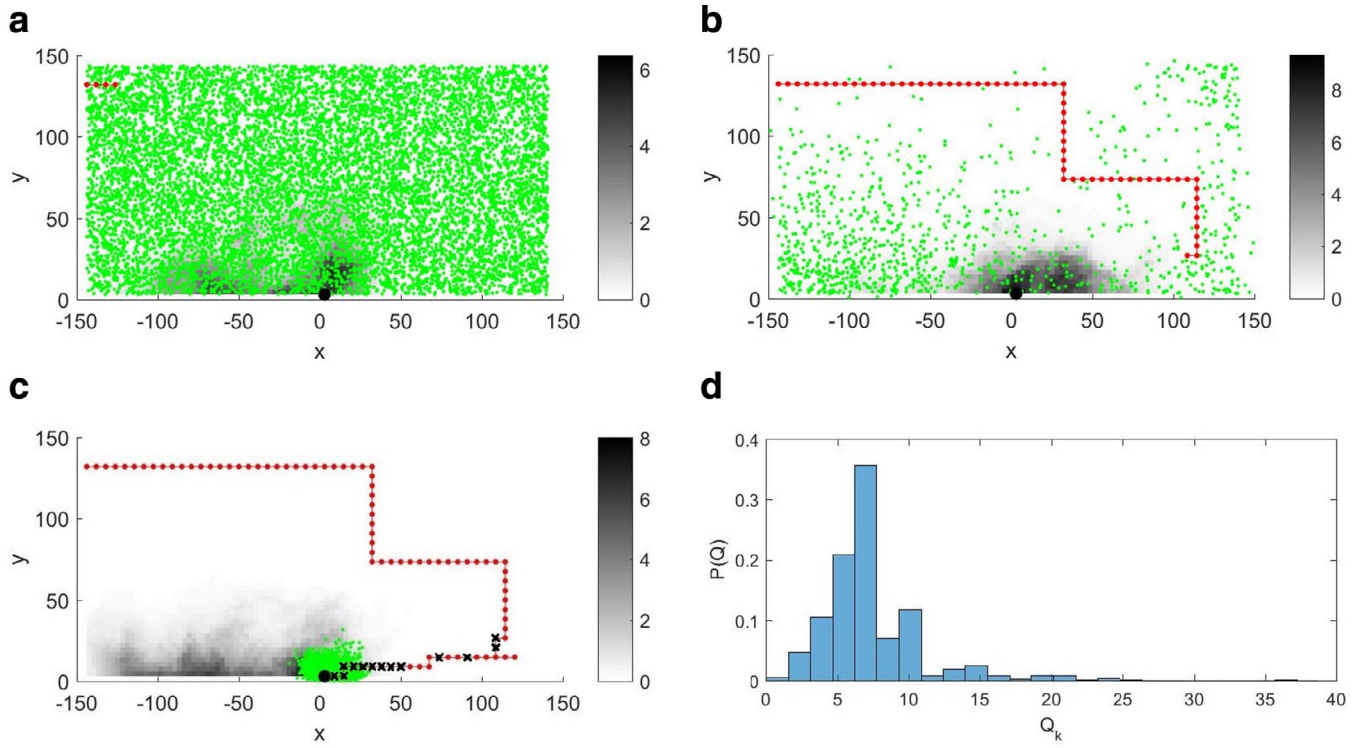

Fig. 6. An illustrative run of the Entrotaxis algorithm at time steps: a) $k = 4$; b) $k = 64$; and c) $k = 90$ using the experimental dataset. The histogram in d) displays the posterior estimate of the source release rate Q_k at the end of the search. Simulation parameters are as follows: $[x_1\ y_1] = [0.67\ 1.67]$, $X_s = Y_s = 2.935$, $v = 0$, $a = 2.935$, $\lambda = \sqrt{1000}$, $N = 10,000$. The true source location is indicated by a large black dot, green dots represent the random samples of the particle filter, the red line indicates the trajectory of the searcher, red dots indicate zero measurements and black crosses non-zero measurements. The greyscale shading depicts the instantaneous concentration field at the current time step. (For interpretation of the references to colour in this figure legend, the reader is referred to the web version of this article.)

Algorithm 1. Entrotaxis.

1: $k = 0$
2: SEARCH = 'ON'
3: **while** SEARCH = 'ON' **do**
4: $k = k + 1$
5: $d_k \leftarrow$ read new sensor measurement
6: $\{(\theta_{k-1}^{(i)}, w_{k-1}^{(i)})_{1\le i\le N} \rightarrow \{(\theta_k^{(i)}, w_k^{(i)})_{1\le i\le N}$ update particle filter
7: **for** all $\mathbf{u}_k \in U_k$ **do**
8: consider potential position $\hat{\mathbf{p}}_{k+1} = (\hat{x}_{k+1}^{\mathbf{u}_k}, \hat{y}_{k+1}^{\mathbf{u}_k})$
9: **for** i = 1:N **do**
10: determine $R\left(\hat{\mathbf{p}}_{k+1}|\theta_k^{(i)}\right)$
11: **for** $j = 1 : d_{\max}$ **do**
12: determine $P(\hat{d}_{k+1}(\hat{\mathbf{p}}_{k+1})|\mathbf{D}_{1:k})$ using Eq. (13)
13: calculate $I(\mathbf{u}_k)$ using Eq. (14)
14: $\mathbf{u}_k^* = \arg\max\{I(\mathbf{u}_k)\} \leftarrow$ new manoeuvre
15: $(x_{k+1}, y_{k+1}) = (x_k, y_k) + \mathbf{u}_k^* \leftarrow$ new position $\mathbf{p}_{k+1}$
16: **if** STOPPING-CRITERIA reached **then** SEARCH = 'OFF'

Table 4
Monte Carlo results using the experimental dataset after 200 runs with various prior distributions for the release rate. (SR = success rate [%]; MST = mean search time [number of measurements]).

Method	$\mathscr{L}(1, 1.2)$	$\mathscr{U}(0, 20)$	$\mathscr{N}(7, 2)$
Entrotaxis			
SR	98	99	99.5
MST	93	93	76
Infotaxis			
SR	99	98.5	99
MST	101	96	80

algorithm was shown to perform marginally better than the original Infotaxis reward by removing bias towards the source. Following the estimation of source parameters, which is carried out using the particle filter as described in Section 4, the Infotaxis II reward selects the manoeuvre that is expected to minimise the entropy of the posterior distribution:

$$I(\mathbf{u}_k) = -\int P(\hat{d}_{k+1}(\hat{\mathbf{p}}_{k+1})|\theta_k) H(\theta_{k+1}|\hat{d}_{k+1}(\hat{\mathbf{p}}_{k+1}), \mathbf{D}_{1:k})\, \mathrm{d}\hat{d}_{k+1}, \tag{15}$$

where the entropy of the posterior $H(\theta_{k+1}|\hat{d}_{k+1}, \mathbf{D}_{1:k})$ is defined as the Shannon entropy:

$$\begin{aligned} &H(\theta_{k+1}|\hat{d}_{k+1}(\hat{\mathbf{p}}_{k+1}), \mathbf{D}_{1:k}) \\ &= -\int P(\theta_{k+1}|\hat{d}_{k+1}(\hat{\mathbf{p}}_{k+1}), \mathbf{D}_{1:k}) \log P(\theta_{k+1}|\hat{d}_{k+1}(\hat{\mathbf{p}}_{k+1}), \mathbf{D}_{1:k})\, \mathrm{d}\theta_k. \end{aligned} \tag{16}$$

The first term in Eq. (15) is the same as Eq. (12). The term $P(\theta_{k+1}|\hat{d}_{k+1}, \mathbf{D}_{1:k})$ in Eq. (16) is solved by updating the current particle filter weightings $w_k^{(i)}$ to pseudo weights $\hat{w}_{k+1}^{(i)}$, that would be produced in response to a hypothesised measurement $\hat{d}_{k+1}$. The overall expected reduction in posterior entropy is computed by a summation over all possible future measurements $\hat{d}_{k+1} = \{0, 1, 2, \ldots, \hat{d}^{\max}\}$:

$$I(\mathbf{u}_k) \approx \sum_{\hat{d}_{k+1}=0}^{\hat{d}^{max}} \sum_{i=1}^{N} P(\hat{d}_{k+1}(\hat{\mathbf{p}}_{k+1})|\theta_k^{(i)}) \hat{w}_{k+1}^{(i)} \log \hat{w}_{k+1}^{(i)}. \tag{17}$$

In terms of computation, both algorithms see an increase in response to higher concentrations which, in turn, cause the value of $\hat{d}^{\max}$ to increase. This is directly caused by the summation over potential measurements seen in both approaches Eqs. (14) and (17). For each potential measurement, Entrotaxis determines its corresponding probability, however Infotaxis must recompute the normalized posterior distribution, resulting in $2N|U_k|\hat{d}^{\max}$ more operations, where $|U_k|$ is the cardinality of manoeuvres U_k. This is caused by extra operations in the innermost for loop of Algorithm 1. The result is 23% faster decision making made by the Entrotaxis algorithm whilst running on an Intel(R) Core(TM) i7-6700HQ 2.60 GHz CPU.

5.2.2. Results

Typical search paths of the Entrotaxis and Infotaxis algorithms searching for a source of various release rates are shown in Fig. 4. The results after 100 Monte Carlo simulations for several values of release rate are provided in Table 1. The results indicate both approaches are adversely affected by weak sensing conditions, however, the Entrotaxis reward performs better in terms of the mean search time (MST). This is supported by the figures which display a more efficient path. The longer MST of the Infotaxis algorithm is due to its tendency to trace the domain boundary. Meanwhile, Entrotaxis would alter its search path sooner in response to the sensory cues. The increase in search time is caused by the larger ratio between the search area and the sensing area as reported in [25]. Essentially, the searcher spends much more time observing null sensor measurements, which are less informative than positive readings.

The algorithm's performance under various mean wind velocity v

conditions were also analysed as subject to constant release rate $Q_s = 2$. Typical search paths executed by Entrotaxis and Infotaxis are shown in Fig. 5, accompanied by Table 2 to summarise the search performance. The table demonstrates the performance benefits of the Entrotaxis algorithm in low wind conditions, particularly as v goes to zero. The Infotaxis algorithm shows consistent performance improvements in response to increasing wind speeds, as was also observed by Ristic et al. [25].

Thus far, the search strategies have considered favourable initial conditions, (with regards to searcher position in relation to the source and the bounds of the domain) where the searcher would start downwind of the source which is positioned near the upwind centre of the domain. These assumptions are not valid for most scenarios seen by humans or in the natural world. In Table 3, we display Monte Carlo search results for various release rate Q_s and wind velocity v combinations, where the source location and searcher starting locations are generated randomly within the domain, i.e. $[x_1\ y_1\ X_s\ Y_s] = \mathscr{U}[0\ 10]$. The remaining parameters are set to the same values as Fig. 1.

The results in Table 3 follow a similar trend to Tables 1 and 2. Both algorithms performed worse in the low release rate conditions. The Infotaxis approach saw a significant improvement in performance in response to increased wind velocity and release rate, although Entrotaxis still had a more rapid MST. In most cases, the MST for both algorithms was lower than previous tables; however, this was expected, as most often the starting positions of the source and searcher would be closer together.

6. Experimental results

We test the Entrotaxis strategy on an experimental dataset which was supplied by the DST Group [25]. The dataset was collected by the COANDA Research and Development Corporation using a large recirculating water channel. Fluoresceine dye was released at a constant rate from a narrow tube at the upwind end of the tunnel. Observations of the concentration of dye were obtained by using laser induced fluorescence. The dataset consists of a sequence of frames denoting the instantaneous concentration field in the vertical plane. Each frame consisted of 49×98 pixels, where each pixel corresponds to a $2.935 \times 2.935\,\text{mm}^2$ area. The nearest integer of a pixel was taken as the number of particle encounters with the sensor at the corresponding position and time. At each time step, the searcher would move to a neighbouring pixel to make an observation. We present a typical run of the Entrotaxis algorithm using the experimental dataset in Fig. 6. The source, located at $[x_s\ y_s] = [2.935\ 2.935]$, is represented by a large black dot. The greyscale shading depicts the instantaneous concentration field at the current time step k, and the histogram in Fig. 6(d) displays the posterior distribution of the source release rate Q_k at the end of the search. The PDF for the release rate using the experimental dataset is of sometimes multimodel, however in the simulated scenarios (Fig. 3(d)) it is monomodal. This is caused by unforeseen mismatches between the modelling and the experimental dataset which can cause multiple modes.

We assess the performance of Entrotaxis on the experimental dataset using 200 Monte Carlo runs. We adopt the simulation parameters used in [25] (including a two dimensional version of the rate of encounters to replace Eq. (1)) as follows: $[x_1\ y_1] = [0.67\ 1.67]$, $X_s = Y_s = 2.935$, $v = 0$, $a = 2.935$, $\lambda = \sqrt{1000}$, $N = 10,000$. A search is terminated if the spread of the posterior approximation falls below 5, the searcher lands on the source, or if the number of time steps k exceeds 1000. A search is considered successful if the distance between the estimated source position and the true source position is less than 10. Table. 4 compares the success rate (SR) and mean search time (MST) of the Entrotaxis and Infotaxis algorithms subject to various prior distributions for the release rate of the source $\pi(Q_0)$. The prior distributions assessed include log-normal $\mathscr{L}(m, \sigma^2)$, uniform $\mathscr{U}(min, max)$ and normal $\mathscr{N}(m, \sigma^2)$ distributions. The table is ordered so that the more favourable priors are on the right hand side.

Whilst there is little difference in the SR of the approaches, the Entrotaxis approach has a faster MST for all the prior distributions. Under the more accurate normally distributed prior on the release rate, both strategies have a considerable reduction in the MST; this is caused by the overall larger prior on the release rate, leading both approaches to alter the search path further from the edge of the domain. The experimental results support the previous findings of Table 2, where Entrotaxis was the most successful strategy in low wind conditions. However, as the source was located very near to the edge of the domain, this was also favourable to the typical trajectories of Infotaxis shown in Fig. 5(b) and (d). The experimental results using the Infotaxis algorithm are noticeably different to those reported in [25]. This is expected to be caused by small differences in data processing, algorithm implementation and in the simulation parameters.

7. Conclusions and future work

The Entrotaxis algorithm has been proposed to perform an autonomous search and reconstruction of an emitting source of unknown strength, in turbulent conditions. The sequential Monte Carlo method was used to estimate source parameters as well as for computation of the reward function. The searcher was guided by following maximum entropy sampling principles. The search paths of Entrotaxis and Infotaxis algorithms were compared in response to various conditions, while Monte Carlo simulations assessed the performance against simulated and experimental data. The results identified similar levels of performance in terms of the success rate of the algorithms, however, favourable conditions were observed for both approaches, with regards to achieving a faster mean search time. Entrotaxis performed better in most of our simulations, especially when subject to low wind conditions or strong release rates. There was less difference in the mean search time of the strategies using the experimental data, where the source was located near to the domain edge. Overall, the Entrotaxis approach typically located the source more rapidly than Infotaxis in our numerical simulations, using a less computationally demanding reward function and without degrading the rate of success. Although this paper focuses on the search for a weak emitting source, undergoing turbulent atmospheric transport, it is envisaged that the Entrotaxis strategy would be effective in most search scenarios where a model of the information source can be provided.

There are several extensions of the algorithm that could yield improved performance and still some limiting assumptions that should be alleviated. Firstly, during our study, Entrotaxis was found to perform less well whilst running simulations using the 2D model for the rate of encounters. This is expected to be caused by strong gradients nearby the source in the model, leading the decision making to be biased upon the expected information calculated from local random samples. We shall study this further in the future. A more efficient search may be achieved by consideration of a larger horizon of manoeuvres or through cooperation among multiple vehicles. The computational advantage of Entrotaxis will be beneficial for these more complex algorithms. Finally, removing assumptions about meteorology and the source could prove beneficial for more realistic scenarios. For example, this study is limited to conditions where there is a constant mean wind and a single source with a constant release rate. In the future, it will be important to expand the work to non-continuous releases, varying meteorological conditions and multiple sources.

Acknowledgements

The authors would like to express their sincere thanks to Dr Branko Ristic and the DST Group for supplying the experimental dataset used in the paper.

This work was supported by the Engineering and Physical Sciences Research Council (EPSRC) grant number EP/K014307/1 and the MOD

University Defence Research Collaboration in Signal Processing. The involvement of Dr Hyondong Oh was supported by the 2017 Research Fund (1.170013.01) of UNIST (Ulsan National Institute of Science and Technology) and Basic Science Research Program through the National Research Foundation of Korea (NRF) funded by the Ministry of Education (2017R1D1A1B03029992).

References

[1] S. Davey, N. Gordon, I. Holland, M. Rutten, J. Williams, Bayesian Methods in the Search for MH370, Springer, 2015.
[2] E. Gelenbe, Y. Cao, Autonomous search for mines, Eur. J. Oper. Res. 108 (2) (1998) 319–333.
[3] T. Furukawa, F. Bourgault, B. Lavis, H.F. Durrant-Whyte, Recursive Bayesian search-and-tracking using coordinated uavs for lost targets, Proceedings 2006 IEEE International Conference on Robotics and Automation, 2006. ICRA 2006. IEEE, 2006, pp. 2521–2526.
[4] A.S. Elstein, A. Schwarz, Clinical problem solving and diagnostic decision making: selective review of the cognitive literature, Br. Med. J. 324 (7339) (2002) 729.
[5] K. Haley, Search Theory and Applications, 8 Springer Science & Business Media, 2012.
[6] P. Kearey, M. Brooks, I. Hill, An Introduction to Geophysical Exploration, John Wiley & Sons, 2013.
[7] T.J. Loredo, J.O. Berger, D.F. Chernoff, M.A. Clyde, B. Liu, Bayesian methods for analysis and adaptive scheduling of exoplanet observations, Stat. Methodol. 9 (1) (2012) 101–114.
[8] M. Hutchinson, H. Oh, W.-H. Chen, A review of source term estimation methods for atmospheric dispersion events using static or mobile sensors, Inf. Fusion 36 (2017) 130–148.
[9] L. Champagne, R.G. Carl, R. Hill, Agent models ii: search theory, agent-based simulation, and u-boats in the Bay of Biscay, Proceedings of the 35th Conference on Winter Simulation: Driving Innovation, Winter Simulation Conference, (2003), pp. 991–998.
[10] M. Müller, R. Wehner, The hidden spiral: systematic search and path integration in desert ants, Cataglyphis fortis, J. Comp. Physiol. A 175 (5) (1994) 525–530.
[11] G.M. Viswanathan, V. Afanasyev, S. Buldyrev, E. Murphy, P. Prince, H.E. Stanley, et al., Lévy flight search patterns of wandering albatrosses, Nature 381 (6581) (1996) 413–415.
[12] N.E. Humphries, N. Queiroz, J.R. Dyer, N.G. Pade, M.K. Musyl, K.M. Schaefer, D.W. Fuller, J.M. Brunnschweiler, T.K. Doyle, J.D. Houghton, et al., Environmental context explains lévy and Brownian movement patterns of marine predators, Nature 465 (7301) (2010) 1066–1069.
[13] G.H. Pyke, Understanding movements of organisms: it's time to abandon the lévy foraging hypothesis, Methods Ecol. Evol. 6 (1) (2015) 1–16.
[14] J. Adler, Chemotaxis in bacteria, Science 153 (3737) (1966) 708–716.
[15] A.M. Reynolds, J.L. Swain, A.D. Smith, A.P. Martin, J.L. Osborne, Honeybees use a lévy flight search strategy and odour-mediated anemotaxis to relocate food sources, Behav. Ecol. Sociobiol. 64 (1) (2009) 115–123.
[16] J.S. Kennedy, D. Marsh, Pheromone-regulated anemotaxis in flying moths, Science 184 (4140) (1974) 999–1001.
[17] R.A. Russell, A. Bab-Hadiashar, R.L. Shepherd, G.G. Wallace, A comparison of reactive robot chemotaxis algorithms, Rob. Auton. Syst. 45 (2) (2003) 83–97.
[18] N. Voges, A. Chaffiol, P. Lucas, D. Martinez, Reactive searching and infotaxis in odor source localization, PLoS Comput. Biol. 10 (10) (2014) e1003861.
[19] J.M. Danskin, A theory of reconnaissance: I, Oper. Res. 10 (3) (1962) 285–299.
[20] E.K. Chong, C.M. Kreucher, A.O. Hero III, POMDP approximation using simulation and heuristics, Foundations and Applications of Sensor Management, Springer, 2008, pp. 95–119.
[21] M. Vergassola, E. Villermaux, B.I. Shraiman, 'Infotaxis' as a strategy for searching without gradients, Nature 445 (7126) (2007) 406–409.
[22] S. Pang, J.A. Farrell, Chemical plume source localization, IEEE Trans. Syst. Man Cybern. Part B (Cybern.) 36 (5) (2006) 1068–1080.
[23] H. Yuyao, S. Cheng, Y. Panpan, L. Xiaokang, Bio-inspired guiding strategy for robot seeking intermittent information source, 2016 13th International Bhurban Conference on Applied Sciences and Technology (IBCAST), IEEE, 2016, pp. 161–166.
[24] A. Eggels, R. Kunnen, B. Koren, A. Tijsseling, Infotaxis in a turbulent 3d channel flow, J. Comput. Appl. Math. 310 (2017) 44–58.
[25] B. Ristic, A. Skvortsov, A. Gunatilaka, A study of cognitive strategies for an autonomous search, Inf. Fusion 28 (2016) 1–9.
[26] C.T. Allen, G.S. Young, S.E. Haupt, Improving pollutant source characterization by better estimating wind direction with a genetic algorithm, Atmos. Environ. 41 (11) (2007) 2283–2289.
[27] P.E. Bieringer, L.M. Rodriguez, F. Vandenberghe, J.G. Hurst, G. Bieberbach, I. Sykes, J.R. Hannan, J. Zaragoza, R.N. Fry, Automated source term and wind parameter estimation for atmospheric transport and dispersion applications, Atmos. Environ. 122 (2015) 206–219.
[28] Y. Wang, H. Huang, L. Huang, B. Ristic, Evaluation of Bayesian source estimation methods with prairie grass observations and Gaussian plume model: a comparison of likelihood functions and distance measures, Atmos. Environ. 152 (2017) 519–530.
[29] B. Ristic, A. Gunatilaka, Information driven localisation of a radiological point source, Inf. Fusion 9 (2) (2008) 317–326.
[30] P. Sebastiani, H.P. Wynn, Maximum entropy sampling and optimal Bayesian experimental design, J. R. Stat. Soc.: Ser. B (Stat. Methodol.) 62 (1) (2000) 145–157.
[31] N. Gordon, B. Ristic, S. Arulampalam, Beyond the Kalman Filter: Particle Filters for Tracking Applications, Artech House, London, 2004.
[32] R.T. Cardé, M.A. Willis, Navigational strategies used by insects to find distant, wind-borne sources of odor, J. Chem. Ecol. 34 (7) (2008) 854–866.